2 Laser scanner measurements of *Trypaea australiensis* mound topography

2.1 Introduction

Decomposition reactions in the sediment are fuelled by the supply of organic matter. An active population of burrowing animals will ensure that organic matter is not simply a thin surface layer, accumulated through sedimentation from the water column. Rather, material may be subducted to considerable depths, or buried rapidly due to the expulsion of sediment from depth. The nature of thalassinidean shrimp burrowing points to both possibilities: sediment expulsion rates from mounds are considerable, so creating high burial rates at the surface; and their deep, permanent burrow structures trap organic matter drawn in by bioirrigation currents or mound collapse. An understanding of the animal mixing processes and rates can aid the estimation of organic matter distribution in the sediment.

Typically, measurements of animal mixing are described in terms of a sediment turnover rate, for which there are a number of estimation methods. Rowden and Jones (1993) identified the three most common methods for measuring sediment turnover in thalassinidean shrimp populations, and discussed the relative advantages and disadvantages of each:

Direct entrapment. A sediment trap positioned over a burrow opening collects ejected material. Rates are expressed as mass (wet or dry) or volume per mound, individual or area per unit time. This is the most commonly used method.

Levelling. An area of mounds is levelled and left for a known period of time. Any new material deposited on the surface is collected or the mound geometry is measured. Rates are expressed as mass or volume per unit area per unit time.

Tracer particles. Labelled sediment (eg. fluorescent dye or paint) is placed at known depth(s) in the sediment. Cores are taken after a known time and the depth distribution of labelled particles measured. Rates are expressed as a deposition depth per unit time.

Rowden and Jones (1993) concluded that these methods are not directly comparable, and can yield vastly different sediment turnover estimates for the same species. Their main recommendations were to use the direct entrapment method, quote rates in terms of dry mass (rather than wet mass or volume), and to use the characteristics of the

measurement to constrain the space and time units (eg. if experiments were conducted over one week, do not extrapolate to yearly estimates).

Problems exist with all three methods. Most importantly, they are all destructive methods in some way. The direct entrapment method removes ejected material and the levelling method has an unknown effect on sediment ejection rates. The tracer particle method needs a sectioned core to obtain just one estimate of turnover rates, so turnover rates as a function of time in one place are not possible and this method is most appropriate over long time scales. A significant advantage of the tracer particle method is that it can measure downward transport.

The present study made estimates of *Trypaea australiensis* (Figure 1.2) sediment turnover rates in the laboratory by using a laser scanner. The laser scanner data allowed the creation of high resolution maps of the sediment surface, and the changes in time could be used to estimate rates of mound volume change. This technique has the advantage of being non-destructive, and it is able to detect both upward and downward transport at the sediment surface.

2.2 Experiment description

A laser scanner was constructed in the Pye Laboratory, CSIRO in the early 1990s (J.H. Taylor, personal communication 1997). Its design was based on the description in Huang et al. (1988), with the main difference being the use of a two-dimensional traversing frame rather than a one-dimensional frame. It had been used to measure high-resolution elevation maps of soil surfaces in erosion studies (unpublished), and had been dismantled. I re-assembled the equipment for these experiments.

The equipment consisted of a low power helium-neon laser, a 35 mm format single lens reflex (SLR) camera with a 50 mm lens, a 256 element photodiode array, a high-precision two-dimensional traversing frame and associated electronics and software. The laser was mounted on the traversing frame and directed vertically downwards onto the sediment, creating a light point on the surface. The camera was mounted at a small angle to the laser and the image of the laser point was focussed onto the photodiode array, which was fitted to the back of the camera (Figure 2.1).

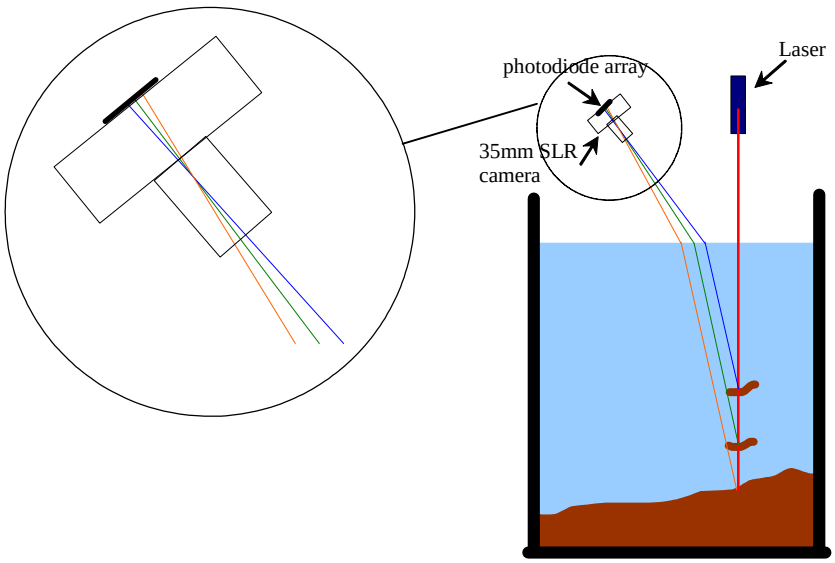

Figure 2.1 Positions of laser and camera relative to the sediment surface. Three possible sediment heights are illustrated to demonstrate the change in image location on the photodiode array. Diagram is not to scale.

The position of the image on the diode array changes if the sediment surface height changes, and so can be used to determine sediment surface elevation. The shape of the image on the diode array could be observed using a cathode ray oscilloscope (CRO). The image was always a bell curve spread across several diodes, and so a method was needed to specify the location of the image centre. Following Huang et al. (1988), a threshold intensity was used to find the extent of the image on the array, and the centre of the image was assumed to lie midway between the first and second threshold crossing. The image position is referred to as the scan count.

In the original article by Huang et al. (1988), analytical equations were given to determine elevation from the scan count, assuming that the absolute positions of the camera and laser are known. In practice, however, better accuracy is obtained by calibrating image positions against a known sediment surface. The calibration approach is better because the geometry of the camera and laser arrangement cannot be determined to the accuracy required. In these experiments, the camera is in air while the sediment is under water, so there is the further complication of refraction at the water surface. The calibration technique avoids these difficulties. The high precision traversing frame was driven by stepper motors, controlled by a Pascal program (authored by Dale Hughes). I modified this program to read in the scan count while traversing.

Four aquaria, each 370 mm × 570 mm, were positioned beneath the traversing frame and filled with sediment sourced from Corunna Lake, a coastal lake near Narooma, NSW, in south-eastern Australia. This lake has a narrow opening to the ocean, and at the time of sampling its tidal sand flats were inhabited by dense populations of thalassinidean shrimp (mainly *Trypaea australiensis*). The sediment and the animals used in the experiments were taken from these tidal flats. Artificial seawater was made up according to standard seawater composition, and a combined pump and filtration system was used to maintain the water quality. The sediment depth was between 25 and 27 cm and the water depth was between 7 and 9 cm in each aquarium. An air conditioner maintained the room at approximately 20 °C.

A calibration ramp was mounted on the inside of one of the walls of each aquarium. The ramp was simply a solid length of plastic, 150 mm in length and 20 mm wide, positioned at an angle to the sediment surface; the uppermost point of each ramp extended out of the water, and the lowermost point extended below the sediment surface level. The ramp elevation was measured relative to the top of each aquarium. Calibration involved traversing the camera and laser over the length of the calibration ramp, so that the image position on the diode array was known over the height range of interest. The scanner, aquaria and calibration ramps are illustrated in Figure 2.2.

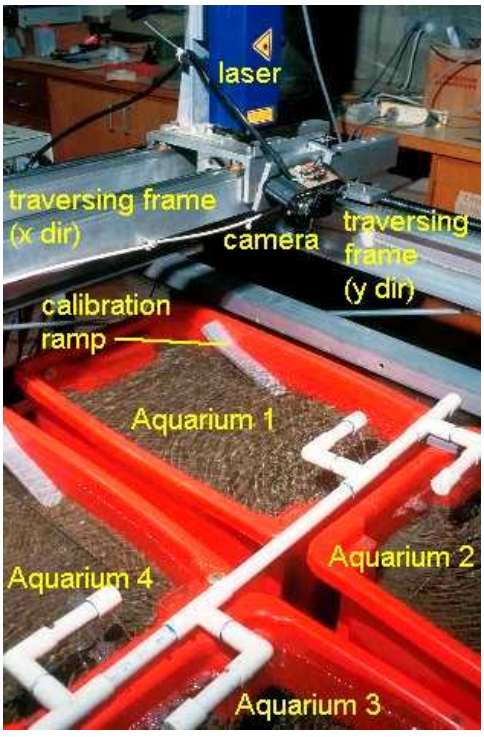

Figure 2.2 Photograph of the laser scanner experimental setup.

Three of the aquaria contained three adult *Trypaea australiensis* individuals each, while the fourth aquarium was left without animals. Each populated aquarium contained one male and two females (sizes given in Table 2.1). The animals were constrained to build their burrows in the centre of each aquarium (a 30 cm by 40 cm area) by the insertion of solid aluminium 'fences'. The fences were needed so that the animals would not burrow near the calibration ramps. Further, measurements could not be made at the edges of the aquaria (aquarium walls blocked the camera's line of sight), so it was more convenient to ensure that the animals were burrowing well away from the walls. The diet of these animals is unknown, but zooplankton was added to the water regularly (usually fortnightly) to ensure fresh organic matter would make its way into the animals' burrows.

Table 2.1 Description of individuals released into each tank. Diameter was measured at the second joint of the abdomen. Length was measured from the eyes to the posterior end of the abdomen.

	Sex	Diameter (mm)	Length (mm)	Wet Mass (g)
Aquarium 1	Male	7.9	40.26	3.26
	Female	8.64	38.85	2.16
	Female	8.35	40.41	2.03
Aquarium 2	Male	8.03	35.74	2.01
	Female	9.15	37.31	2.01
	Female	9.29	42.56	1.99
Aquarium 3	Male	8.34	36.79	2.58
	Female	8.45	42.45	2.21
	Female	8.5	40.48	2.46

Each aquarium scan comprised 161 lines, 420 mm long and separated by 2 mm. The spatial resolution was 1 mm along a scan line. The detection resolution was actually much finer than 1 mm. The scanner on average detected 18 points over each millimetre section (standard deviation of < 4 points), but only the average scan count over each 1 mm section and the number of points forming this average were saved. One scan produced two files, each containing 161 × 420 elements. Scanning time for each aquarium was 1.5 hours, so at least 6 hours were needed to scan all four aquaria.

Before each scan, the camera focus was altered to get the sharpest signal on the CRO. Calibration was required prior to each scan and a post-scan calibration was conducted so that an estimate of drift over the experiment could be obtained.

Scans were usually separated by approximately a fortnight, but there were periods of more frequent scanning on Aquarium 1. The sediment surface was cleared of all mounds on Day 111 so that recovery from surface disturbance could be observed.

Analysis was divided into two time periods. Time Period 1 is Day 1 to Day 110, and Time period 2 is Day 111 to Day 359.

2.3 Data Analysis

All data analysis was conducted in Matlab. Analysis comprised calibration, map construction and individual mound analysis, as described in the following three sections.

2.3.1 Calibration

Calibration ramp elevation was measured at known y-values by traversing the laser to a y-location, and then measuring the vertical distance from the top of the aquarium to the laser point on the ramp. Five or six points were measured on each ramp, and linear relationships were found to describe ramp elevation (z) as a function of y ($R^2>0.9995$). The locations of the calibration ramps were measured either two or three times during the first two weeks of experiments, and again at the end of all experiments just under a year later. Measured values within the first two weeks differed by at most 0.5 mm, and after a year the ramp locations had changed by at most 1.5 mm, and were more typically under 0.5 mm from original measurements.

At the beginning and end of each aquarium scan, the calibration ramps were scanned five times, producing scan count values for known y locations. (In four cases, one of the ten ramp scans produced a spurious scan count. These four values were replaced with an average of their two neighbours. In one case, a 'bump' was clear on all 10 scans of a calibration ramp, and so seven points were removed from all 10 scans to remove the bump.) The values across the ten scans were averaged, the elevations at these locations were calculated from the linear relationship described above, and a third order polynomial fit was found relating elevation (z) to scan count (c). There were 53 scans of Aquarium 1 and 33 of the other three aquaria, so 152 calibration polynomials were produced using this technique. Residuals were calculated by taking the absolute value of the difference between ramp elevations and elevations calculated from the third order polynomial. The mean residual was 0.18 mm (n = 145590, standard deviation = 0.17 mm), and the maximum residual was 1.09 mm.

2.3.2 Map construction

Raw scan count files were converted to elevation using the calibration polynomials. Spurious points (elevations outside the calibration range) were identified and replaced

with interpolated functions (Matlab's *interp2* function, using the bicubic interpolation method). The worst scan (requiring many such replacements with interpolated values) is shown in Figure 2.3. In this case, specks of dirt were floating on the water surface, and so interfered with the scan (the laser point would either intersect the particles, or it would be refracted when passing the meniscus surrounding the floating particles). The surface water was checked and cleared of debris in all subsequent scans, so this problem was an isolated event.

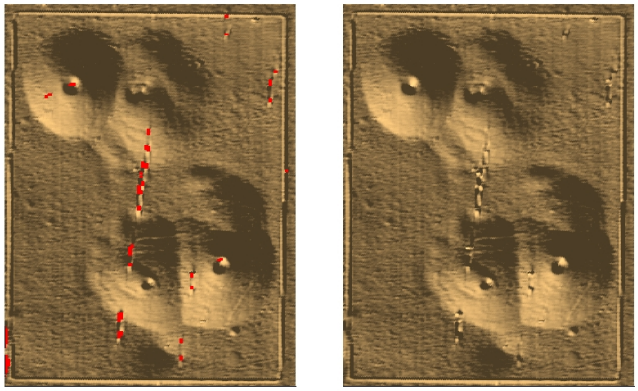

Figure 2.3 Left hand image: surface reconstruction from raw elevation data (red patches mark out-of-range elevations). Right hand image: filtered elevation data (out-of-range values replaced with interpolated values). This particular example was the worst case. Most out of range values were due to particles floating on the water surface, and this problem was eradicated in subsequent scans.

The resulting elevation files are readily viewed as three-dimensional maps and animation sequences. Surface maps for each aquarium are shown in Figure 2.4 to Figure 2.7. The figures have been generated in Matlab using the 'surf' function. The shadows in the images (due to a simulated light source) are to assist three-dimensional mound visualisation. Elevation is quoted relative to the aquarium top in all cases.

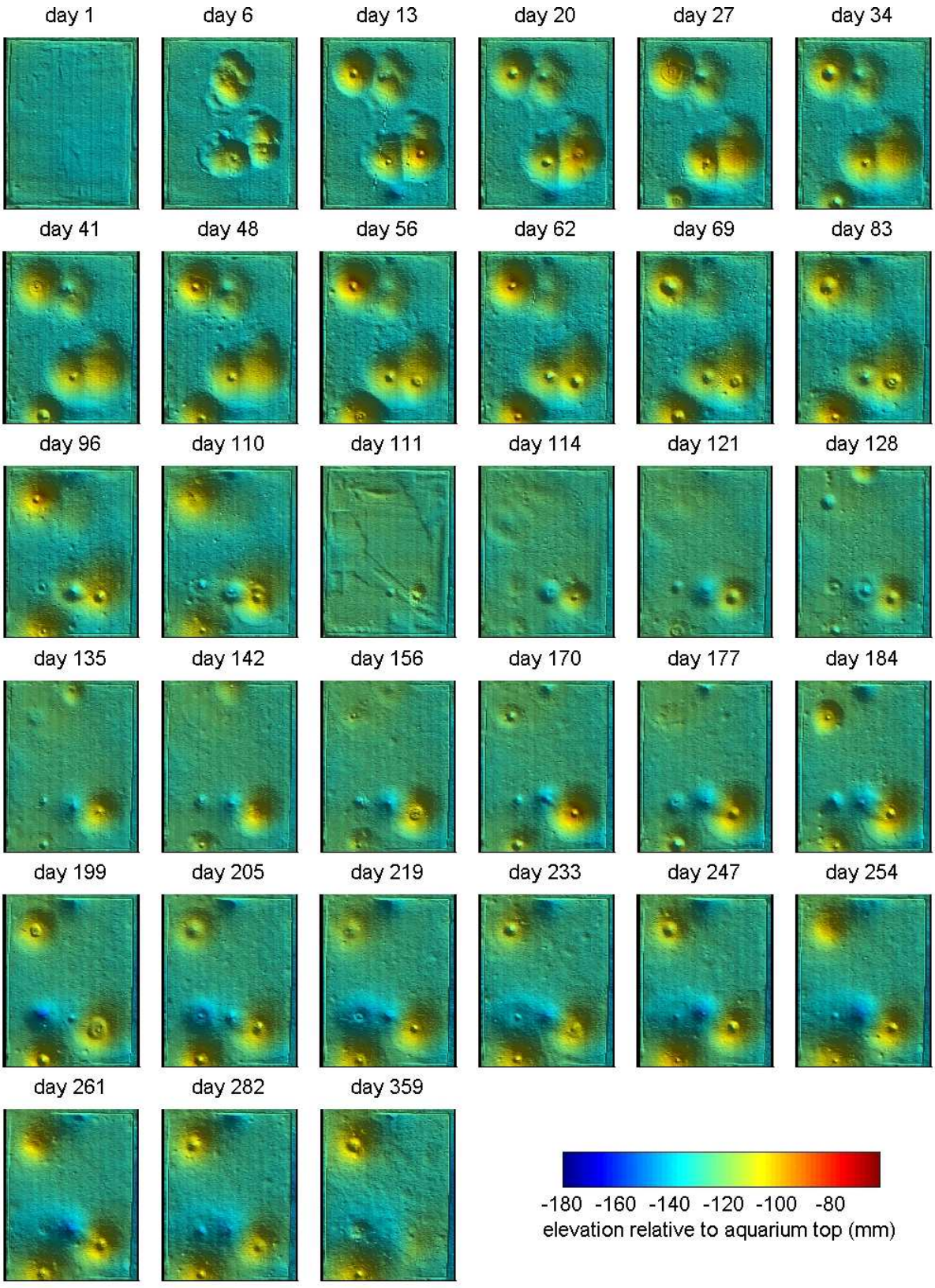

Figure 2.4 Aquarium 1 elevation maps. Some maps excluded for ease of comparison with other aquaria, and are shown in Figure 2.20.

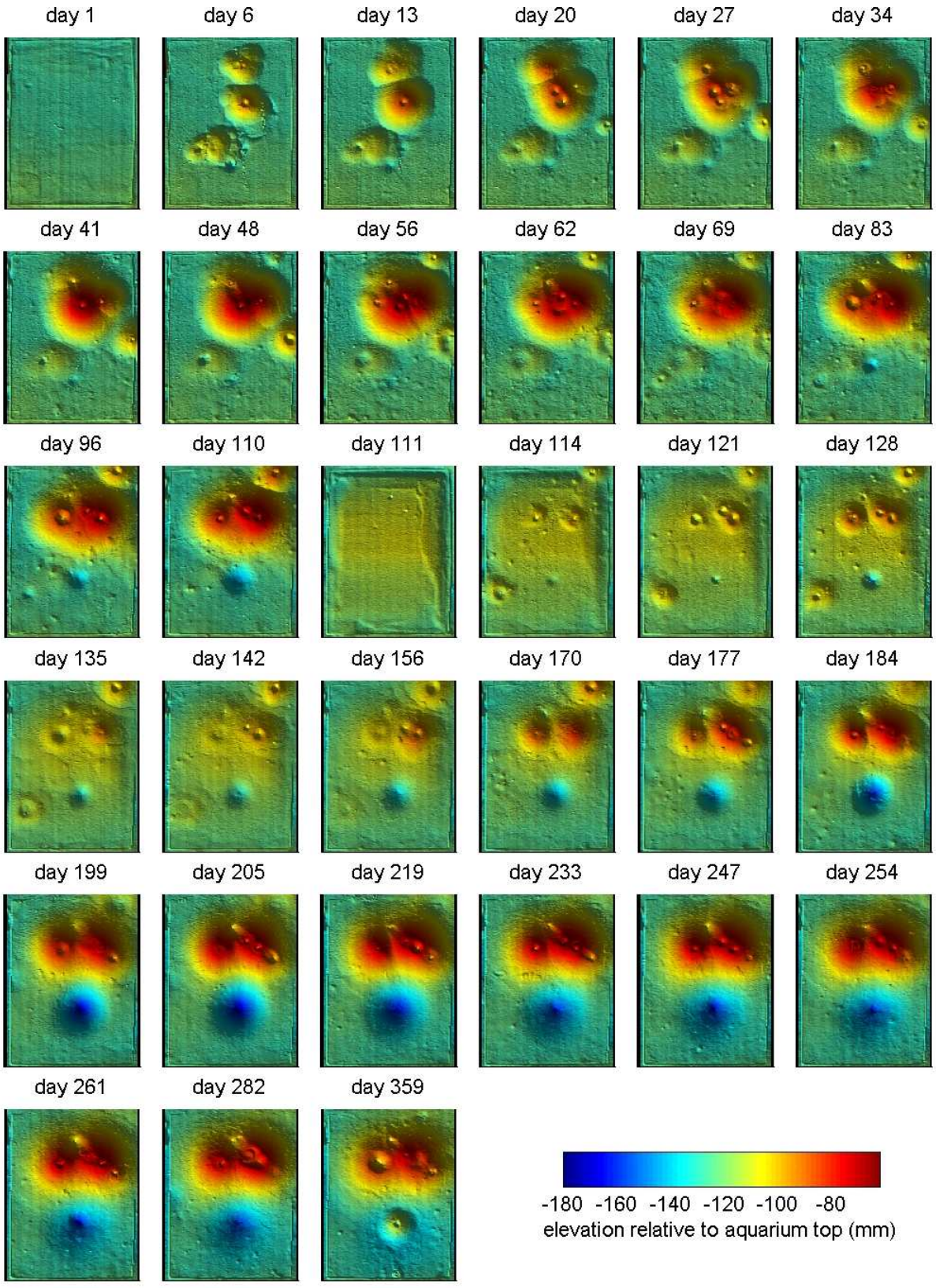

Figure 2.5 Aquarium 2 elevation maps.

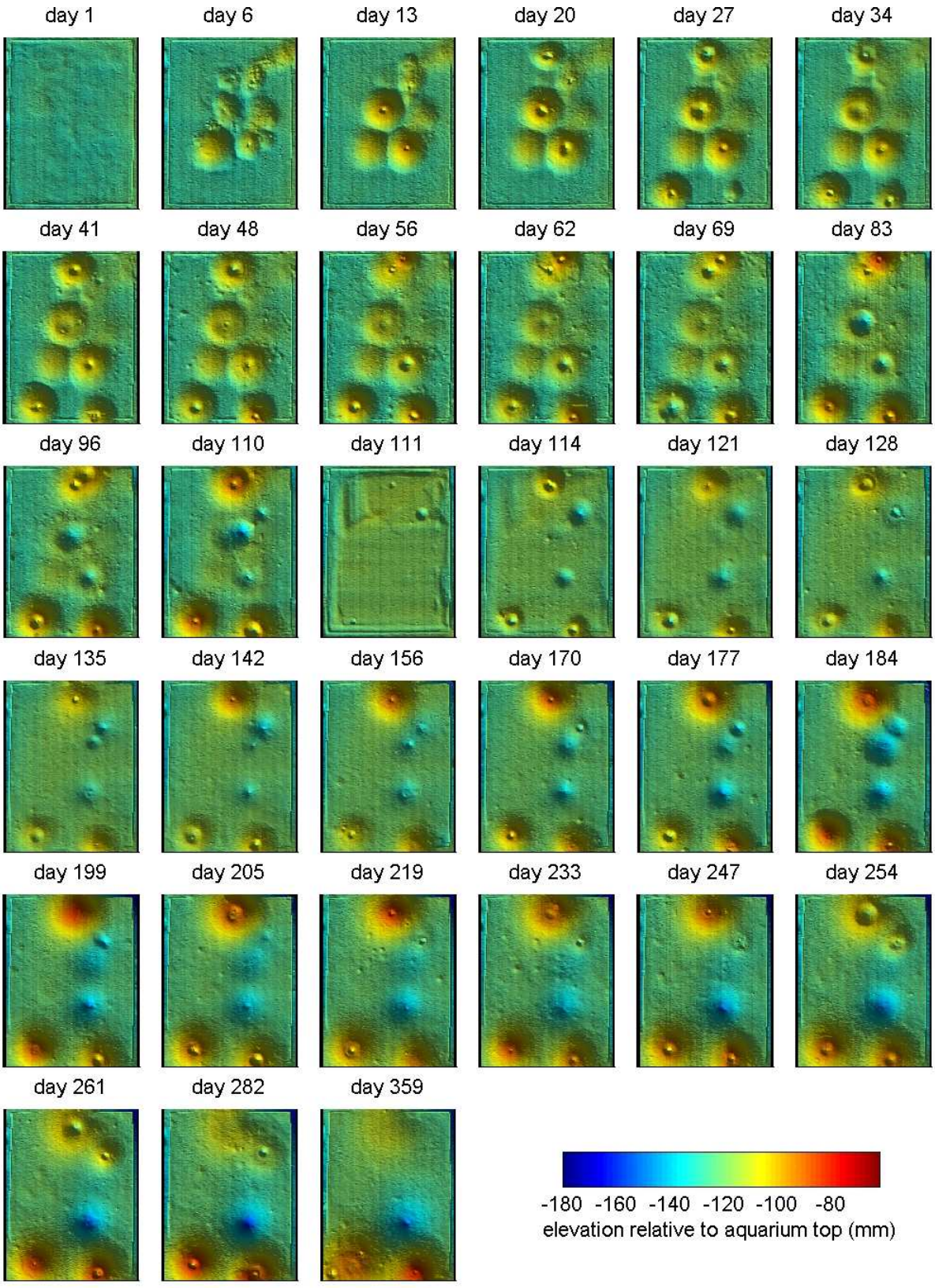

Figure 2.6 Aquarium 3 elevation maps

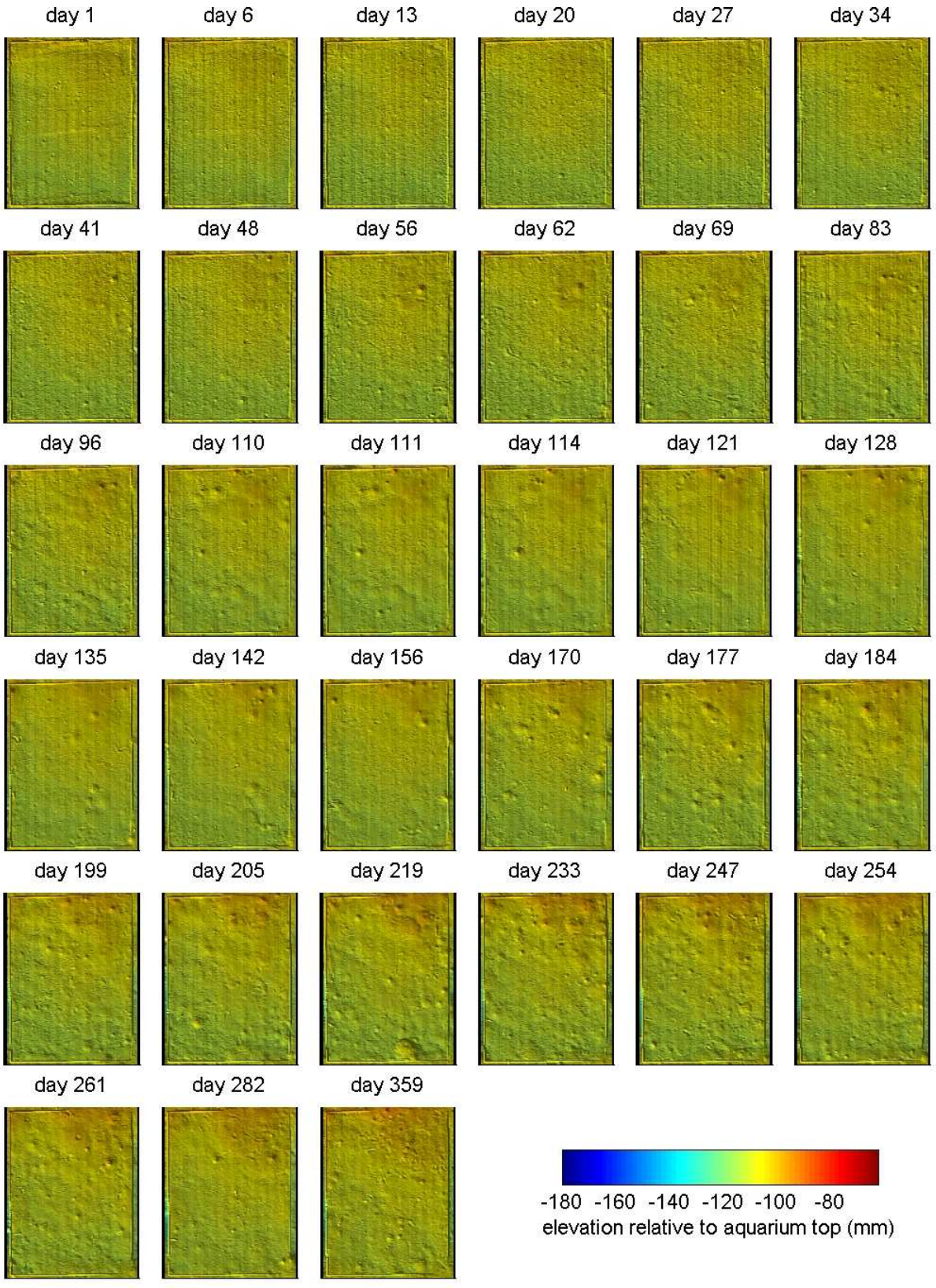

Figure 2.7 Aquarium 4 elevation maps.

2.3.3 Individual mound analysis

Although three individuals were added to each aquarium, it was uncertain how many animals were alive throughout the experiment. In the field, too, mounds can be identified easily but the relationship between the number of mounds and the number of individuals is unknown (McPhee and Skilleter (2002)). For these reasons, volumes and rates of change of volumes were calculated for each mound without attempting to assign them to individual animals.

Mound regions were identified by tagging locations that experienced elevation changes of >15 mm over the measurement period of interest. Matlab was used to generate lines showing the 15 mm contour (Figure 2.8), and then contour lines were edited manually to close polygons and to split some regions into separate mounds, where possible (Figure 2.9). All mound regions were defined to lie within the 'fenced' area. Volume changes were calculated within the mound regions using trapezoid numerical integration. Some mounds spilled material over the fence, and so volume estimates for these mounds are an underestimate.

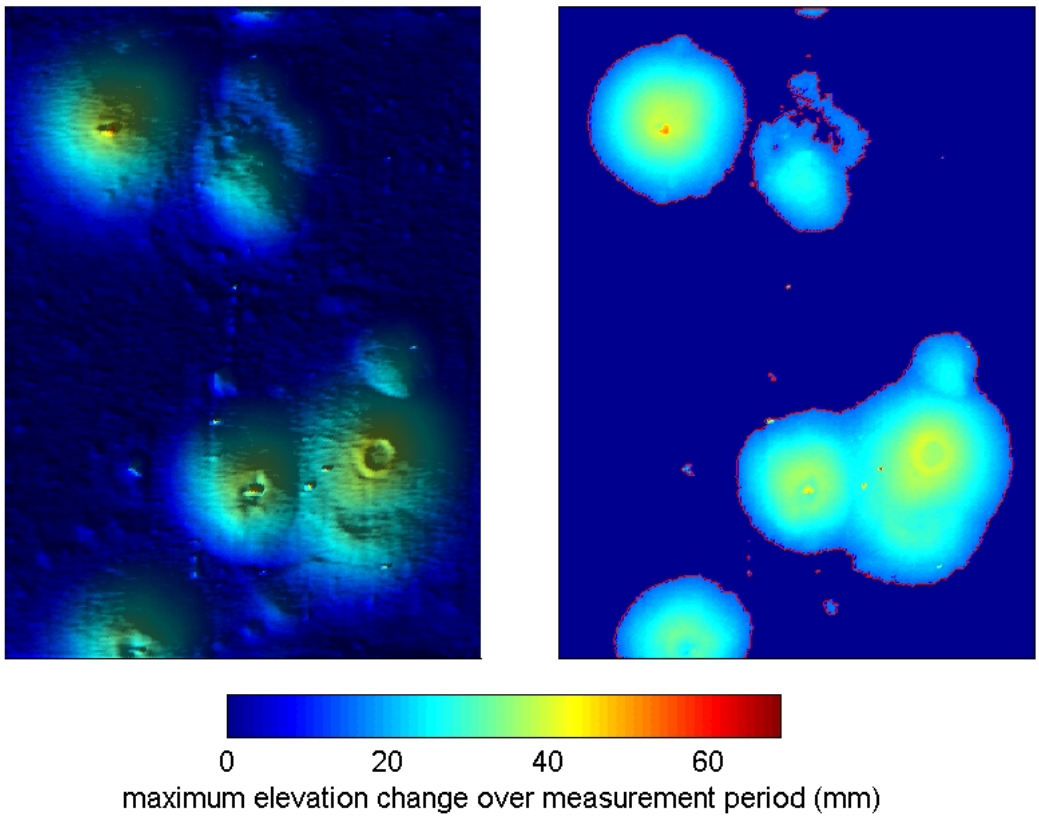

Figure 2.8 The left-hand image shows the maximum change in elevation in Aquarium 1, over Time Period 1 (Day 1 to Day 110). The right-hand image shows the same data, with the 15 mm contour line in red. All data values below 15 mm are coloured dark blue (0 mm) to accentuate mound regions.

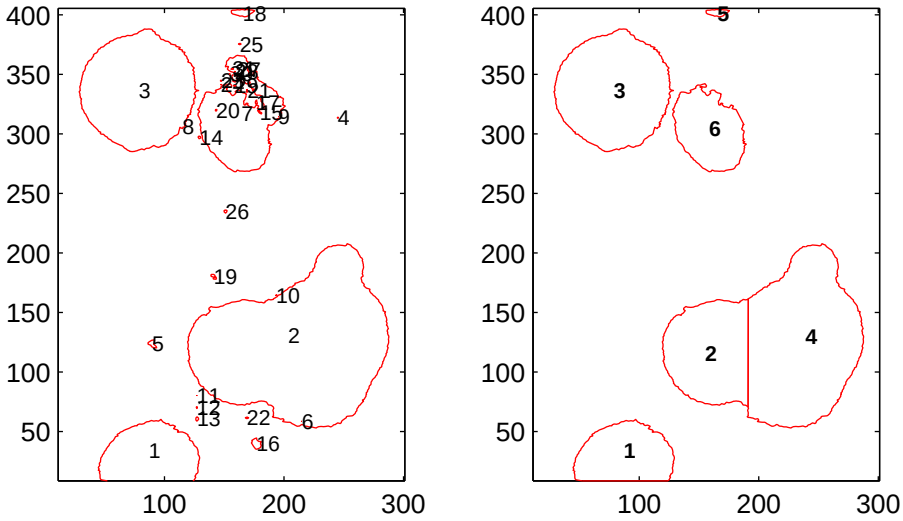

Figure 2.9 The left hand side shows the raw mound regions calculated from Figure 2.8 (Aquarium 1, Time Period 1), and the right hand figure shows the final mound regions after manual editing. Polygons have been closed (eg. lower edge has been added to Mound 1), and mound regions have been split (eg. compare Mound 2 on LHS and Mounds 2 and 4 on RHS). Small regions not obviously associated with a mound have been removed (eg. Mound 26 on LHS).

Once mound regions had been identified for each time period, the locations of burrow openings were found for each scan. A Matlab script was used to loop through images of each mound at each scan, and the mouse was used to identify burrow openings for each scan image. All mounds and their openings for each time period are shown in Figure 2.10. The mound area and average (mode) number of openings for all mounds are given in Table 2.2.

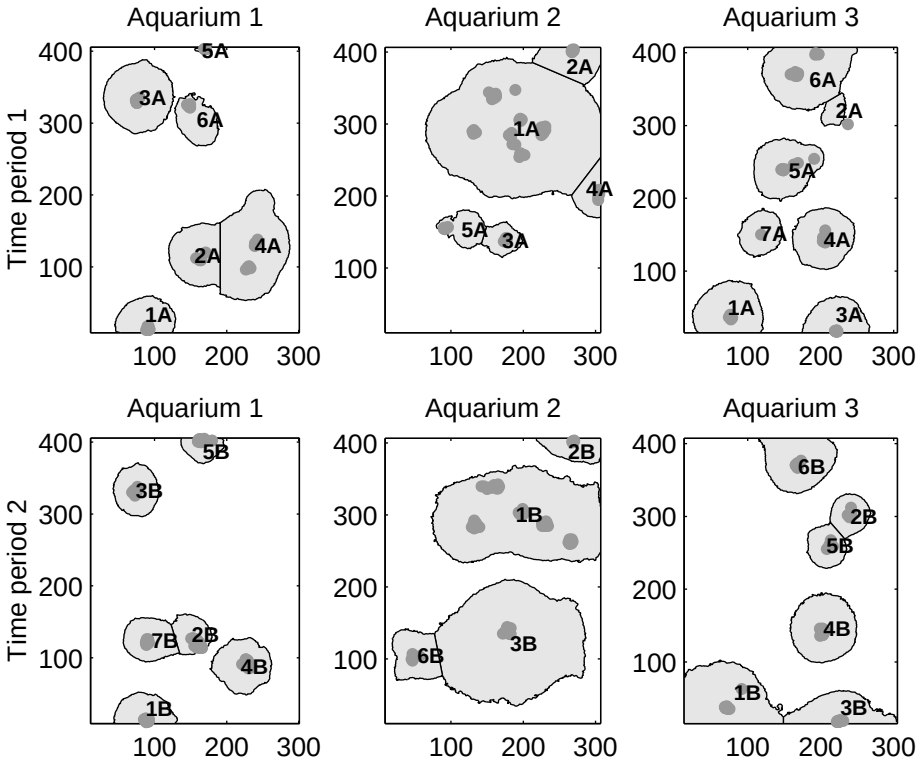

Figure 2.10 Mound regions for each aquarium and time period. Dark grey circles mark all hole locations that existed during the lifetime of each mound. (Time period 1: day 1 to day 110; Time period 2: day 111 to day 359.) Axis dimensions are mm.

Table 2.2 The area and the average (mode) number of openings for each mound. Letters A and B denote Time Period 1 and 2 respectively.

	Aquarium 1		**Aquarium 2**		**Aquarium 3**	
Mound region	*Average number of openings (mode)*	*Area (cm^2)*	*Average number of openings (mode)*	*Area (cm^2)*	*Average number of openings (mode)*	*Area (cm^2)*
1A	1	33.96	4	360.01	1	56.66
2A	1	53.64	1	34.43	1	11.26
3A	1	73.91	1	18.37	1	34.4
4A	1	111.57	1	20.07	1	55.27
5A	1	0.82	1	23.22	1	59.42
6A	1	31.03	-	-	1	85.58
7A	-	-	-	-	1	28.67
1B	1	28.85	5	255.23	1	90.24
2B	1	23.27	1	23.2	1	24.16
3B	1	35.3	1	268.46	1	45.01
4B	1	47.66	1	0	1	67.34
5B	1	15.53	1	0	1	24.96
6B	1	0	1	39.52	1	61.05
7B	1	36.63	-	-	-	-

2.4 *Results and discussion*

2.4.1 General Observations

The sediment was not sieved prior to filling the aquaria, so other small life-forms were present in the sediment. The sediment was sorted by hand to remove any obvious macrofauna (mainly molluscs), but small worms and meiofauna remained. Their presence explains the changes in sediment surface observed in Aquarium 4, and away from mound regions in the other aquaria. The burrow openings to the shrimp burrows are unmistakable, and are easy to distinguish from the smaller surface changes caused by other organisms.

Burrow openings, once formed, tended to remain in place in undisturbed conditions. Clearing the surface on Day 111 prompted more dramatic changes, but the general position of the burrow openings remained largely unchanged.

Individual mounds were observed in Aquaria 1 and 3, however Aquarium 2 was quite different. Many burrow openings were concentrated into a relatively small area, creating a 'giant' mound comprising many holes (Figure 2.11). Further, the holes in this mound were less permanent.

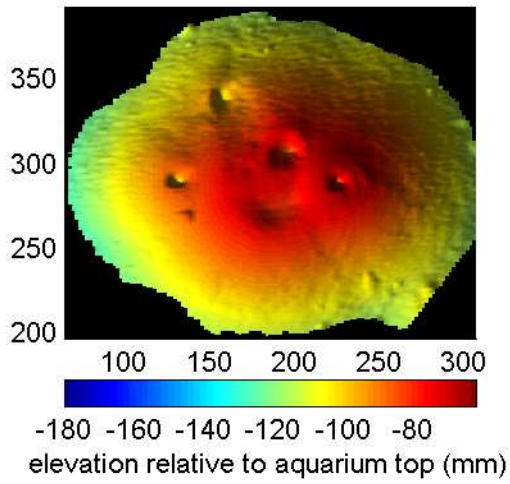

Figure 2.11 Example of a 'giant mound' comprising many burrow openings. (Aquarium 2, Day 62, Mound 1A. Axis units are mm.)

Burrow openings were observed to open and close regularly, and considerable downward transport of sediment surface into burrows was apparent. Some mounds were observed to collapse and change into funnels over time (eg. Figure 2.12). Some openings never formed a mound, and so were sites of downward transport only.

Where a mound and a funnel were close to one another, mound material was observed to move down into the neighbouring funnel (eg. Figure 2.13).

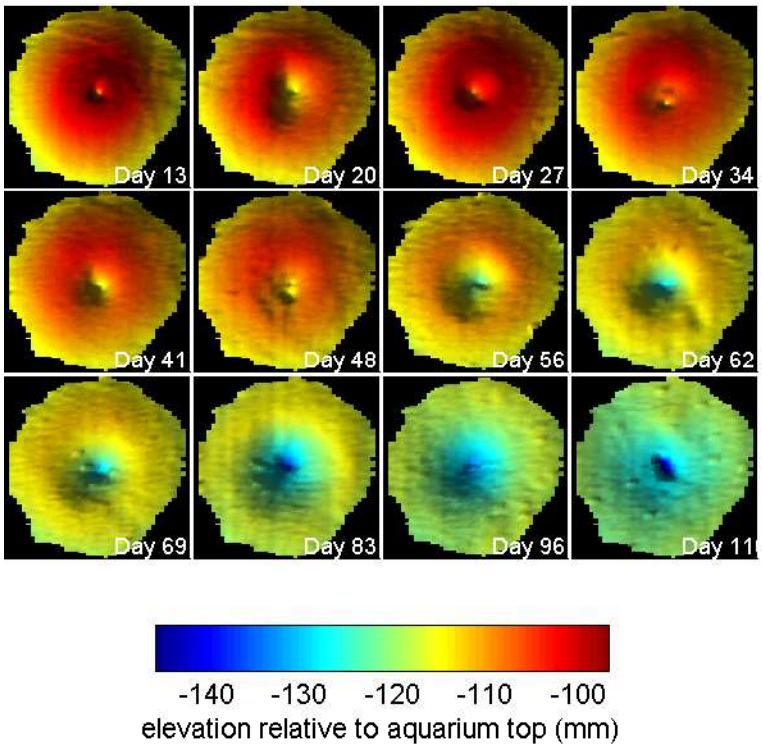

Figure 2.12 Example of a mound changing into a funnel. (Mound 4A in Aquarium 3).

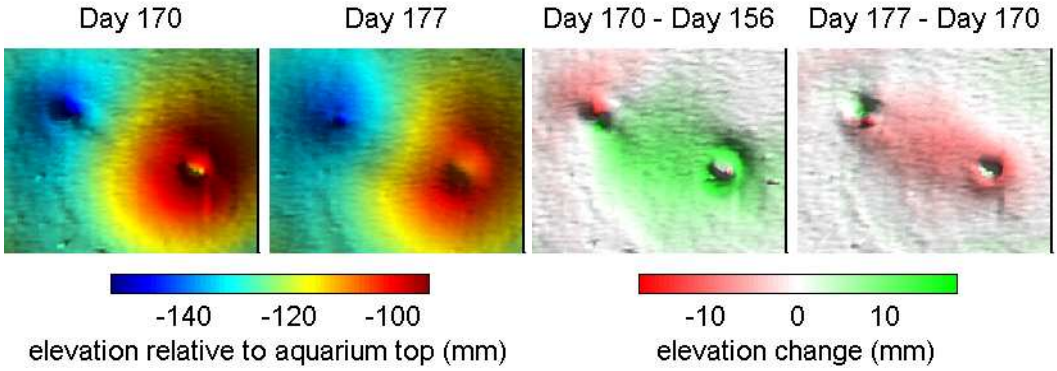

Figure 2.13 Example of mound material falling into neighbouring funnel. (Aquarium 1, Mounds 2B & 4B, Time Period 2). The two left hand figures show the surface maps, and the two right hand figures show the difference in elevation between two maps. White regions are regions of negligible elevation change, green regions show a rise in surface elevation and red regions show a fall in surface elevation.

It is clear from these observations that the burrow openings are sites of relatively rapid two-way exchange of solid material between the surface and depth. In the following

section, the scan data is used to calculate rates of transport associated with these surface changes.

2.4.2 Volume estimates

The volume change from scan to scan was calculated for each mound region. The rate of volume change could then be expressed as a volume per mound per unit time. Elevation rises at some coordinates and falls at locations within any mound region, so volume changes have been grouped into three categories:

1. volume expulsion (calculated from points experiencing an elevation increase between adjacent scans);

2. volume subduction (calculated from points experiencing an elevation decrease between adjacent scans); and

3. net elevation change (volume expulsion + volume subduction).

Figure 2.14 shows the cumulative volume change for each mound region. The mean rates of change of volume (cm^3/day/mound region) are given in Table 2.3. These rates were calculated by dividing the final cumulative volume changes for each mound (expulsion, subduction and net) by the number of days, and taking the mean of all mounds.

Table 2.3 Mean rates of volume expulsion, volume subduction and net volume change per mound for each aquarium and each time period (cm^3/day/mound region).

		Mean rate of volume expulsion (std dev) cm^3/day/mound region	Mean rate of volume subduction (std dev) cm^3/day/mound region	Mean rate of volume change (std dev) cm^3/day/mound region
Time Period 1	Aquarium 1	1.38 (1.11)	-0.6 (0.4)	0.78 (0.76)
	Aquarium 2	2.98 (5.56)	-0.58 (0.73)	2.41 (4.86)
	Aquarium 3	1.27 (0.86)	-0.56 (0.38)	0.71 (0.7)
Time Period 2	Aquarium 1	0.39 (0.29)	-0.36 (0.25)	0.03 (0.14)
	Aquarium 2	0.83 (1.39)	-0.8 (1.12)	0.03 (1.25)
	Aquarium 3	0.51 (0.36)	-0.39 (0.23)	0.11 (0.45)

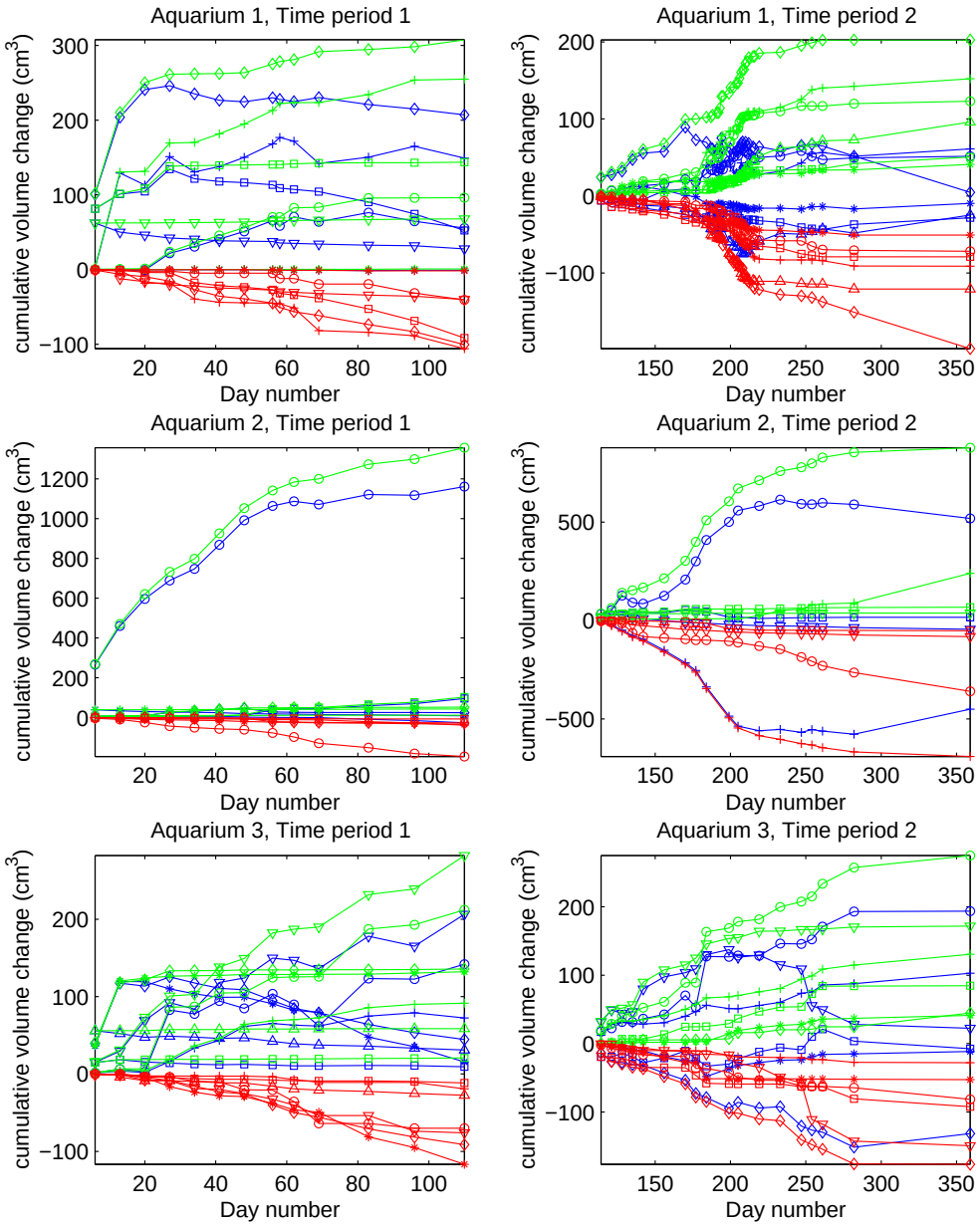

Figure 2.14 Cumulative volume graphs for each mound region within each aquarium and time period (Table 2.2). Each line within a colour group is a single mound region. Green lines show the cumulative volume expulsion, red lines show the cumulative volume subduction and the blue line is the cumulative net volume change (the sum of expulsion and subduction). The marker shape indicates mound region (Mound 1: circle; Mound 2: square; Mound 3: plus; Mound 4: diamond; Mound 5: star; Mound 6: triangle (down); Mound 7: triangle (up)).

This straightforward computation neglects many other considerations. Firstly, the giant mound in Aquarium 2 (Mound 1) was an agglomeration of many mounds, so the rate of volume change for this mound far exceeded the rate for other mounds. Defining a robust set of criteria for splitting the region into individual mounds is not possible,

and so the best that can be done is to estimate the number of mounds in the giant by counting the average (mode) number of openings that exist and normalising the mound volume rate estimate by the number of openings.

Another problem is that it is clear that there was a 'start-up' effect at the beginning of the experiment. The rate of sediment ejection in the first weeks is far greater than in subsequent weeks. The 'start-up' effect is presumably due to the initial construction of a new burrow. Following this initial burrow construction, volume changes are most likely due to routine burrow maintenance, feeding and burrow extension. Forster and Graf (1995) reported that *Callianassa subterranea* specimens were observed to extend their burrows continuously for periods of over a year. Stamhuis et al. (1996) measured behaviour and time allocation of *Callianassa subterranea* in laboratory aquaria and found that 27% of animals' time was spent burrowing (defined as any interaction with the sediment and transport activities – stirring, lifting, carrying, dropping ,tamping, bulldozering, pumping – and would include feeding). Stamhuis et al. (1997) measured the total length of *Callianassa subterranea* tunnel systems over time, and found that initial burrowing velocity (increase in total burrow length per hour) was much higher for the first approximately four days of new burrow construction.

Figure 2.15 shows the same data split into three time periods (Time period 1 split into a start-up period (three weeks) and a subsequent lower growth period), and the data has been normalised by the average (mode) number of openings in each mound at each time step. The data from Day 359 have been excluded; 77 days elapsed between the second last and last scan (Day 282 and Day 359), whereas the usual interval between scans had been no longer than three weeks. These data were used to calculate mean rates of volume change per burrow opening for three time periods (Start-up period, remainder of Time Period 1 and Time Period 2). The results are shown in Table 2.4.

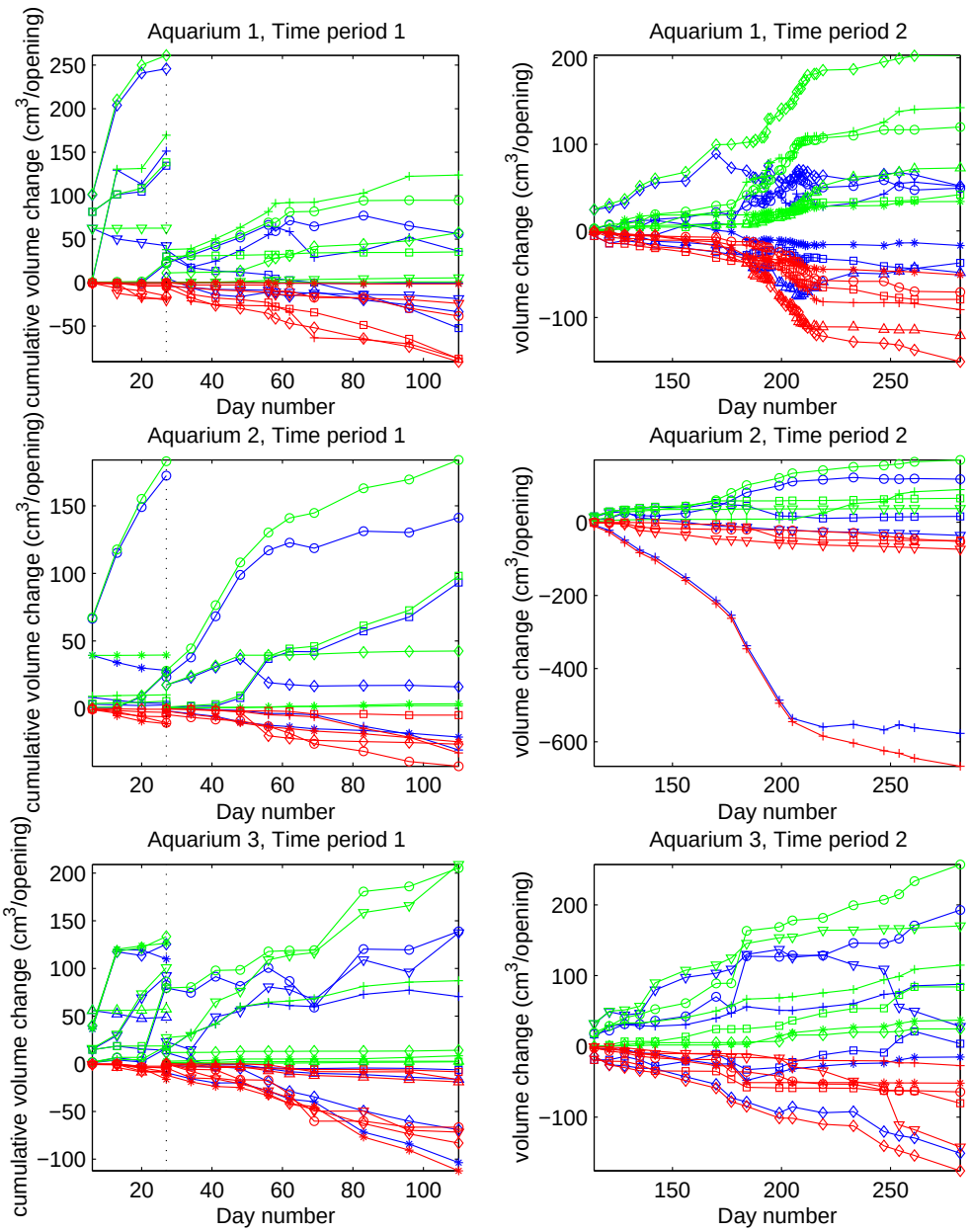

Figure 2.15 Same data as Figure 2.14, normalised by the number of holes in each mound region. Time period 1 has been split into a start-up period (three weeks) and a subsequent period. The colour code and markers are the same as Figure 2.14.

Table 2.4 Mean rates of volume expulsion, volume subduction and net volume change per opening for each aquarium and each time period (cm^3/day/burrow opening).

		Mean rate of volume expulsion (std dev) cm^3/day/opening	Mean rate of volume subduction (std dev) cm^3/day/ opening	Mean rate of volume change (std dev) cm^3/day/ opening
Time period 1a (start-up)	Aquarium 1	4.97 (4.5)	-0.45 (0.41)	4.51 (4.29)
	Aquarium 2	2.41 (3.36)	-0.29 (0.21)	2.12 (3.24)
	Aquarium 3	3.52 (2.15)	-0.34 (0.21)	3.18 (2.01)
Time period 1b	Aquarium 1	0.63 (0.58)	-0.65 (0.46)	-0.02 (0.5)
	Aquarium 2	0.79 (0.91)	-0.31 (0.17)	0.47 (0.89)
	Aquarium 3	0.9 (1.13)	-0.64 (0.47)	0.26 (1.15)
Time period 2 (excluding Day 359)	Aquarium 1	0.52 (0.42)	-0.48 (0.29)	0.04 (0.26)
	Aquarium 2	0.36 (0.38)	-0.83 (1.54)	-0.47 (1.47)
	Aquarium 3	0.68 (0.52)	-0.53 (0.34)	0.14 (0.68)

Strong sampling frequency dependence is apparent in the data. Aquarium 1 was scanned more frequently than the other aquaria between Day 184 and 219 (Time Period 2), and the cumulative volume change graph is markedly steeper during this time period (see Figure 2.15, Aquarium 1, Time Period 2). I calculated the mean rate of volume change per unit area between scans in all mound regions, and plotted them against the time interval between scans (Figure 2.16). Rates of volume change increase with decreasing time interval.

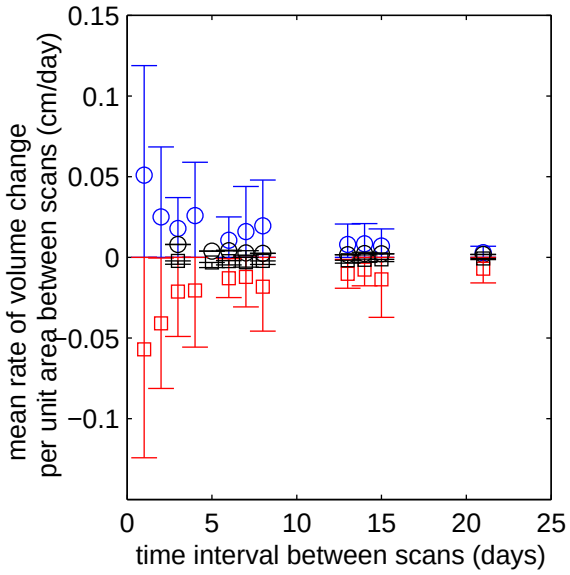

Figure 2.16 Mean rate of volume change per unit area between scans. Circles are sediment accumulation data, squares are sediment subduction data. Blue and red markers are data from mound regions in Aquaria 1 to 3, black markers are data from the unpopulated Aquarium 4. Error bars indicate ± 1 standard deviation.

This pattern is consistent with an aliasing effect. For example, if the surface elevation h were to rise and fall in a sinusoidal pattern according to the following equation:

$$h = A\sin\left(\frac{2\pi}{T}t\right) \qquad \textbf{(2.1)}$$

where t is time (days), A is the amplitude (cm) and T is the period of oscillation (days), the rate of volume expulsion per unit area would be 2A/T cm/day, the rate of volume subduction per unit area would be –2A/T cm/day, and the net rate would be 0 cm/day (Figure 2.17).

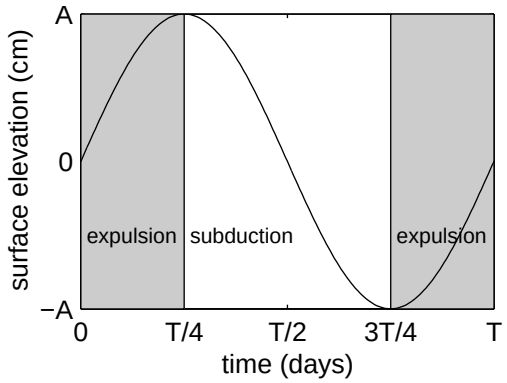

Figure 2.17 Surface elevation rising and falling according to equation (2.1). Sediment is being expelled during the first and last quarter, and subducted during the middle two quarters, as indicated by shading.

If this surface were to be measured infrequently, the calculated volume rates would be a strong function of sampling interval. For example, Figure 2.18 shows the calculated volume expulsion and subduction rates per unit area for different sampling intervals (surface elevation is given by equation (2.1), with A = 1 mm and T = 2 days). The behaviour is the same as that observed in Figure 2.16.

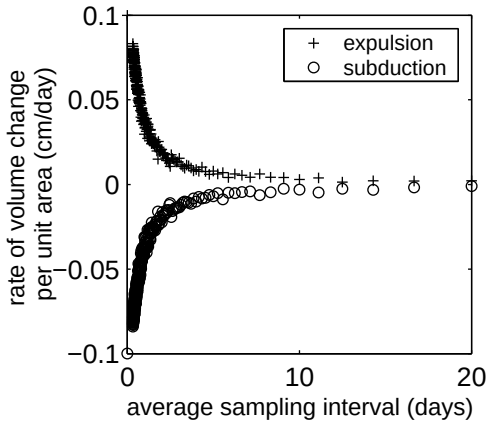

Figure 2.18 The rate of volume expulsion and subduction calculated from sampling an oscillating surface randomly in time over 100 days at a range of sampling frequencies. The surface elevation is given by equation (2.1), with A = 1 mm and T = 2 days.

The impact of sampling interval on rates of volume change is substantial. Figure 2.19 shows the same scan data sampled at different frequencies (Aquarium 1, Days 184 to 219). During this period of time, Aquarium 1 was sampled more frequently than the other aquaria (typically daily, with some exceptions). The other aquaria were only sampled on Days 184, 199, 205 and 219. The rates of volume change from these two scenarios are given in Table 2.5. The calculated rates are 3 or 4 times higher than those calculated from the same data sub-sampled on days 184, 199, 205 and 219. (The rates of net volume change remain the same as this is determined only by the first and last scan of the sampling period.)

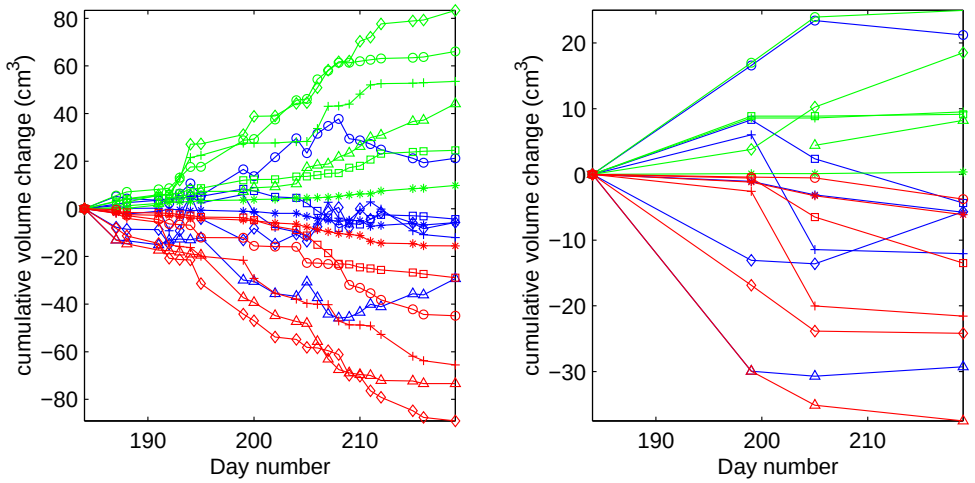

Figure 2.19 Cumulative volume changes for Aquarium 1, Days 184 to 219, sampled at different frequencies. Left hand graph: all data; Right hand graph: the same data sampled less frequently (at the same frequency as the other aquaria). The colour code and markers are the same as Figure 2.14.

Table 2.5 Influence of sampling frequency on calculated mean rates of volume change.

	Mean rate of volume expulsion (std dev) cm^3/day/opening	Mean rate of volume subduction (std dev) cm^3/day/ opening	Mean rate of volume change (std dev) cm^3/day/ opening
Frequent sampling	1.12 (0.84)	-1.26 (0.9)	-0.14 (0.42)
Infrequent sampling	0.28 (0.25)	-0.42 (0.37)	-0.14 (0.42)

Figure 2.20 shows the maps constructed from the frequent scans of Aquarium 1. It is clear from these maps that the mound holes open and close on a daily basis, creating an oscillating change in elevation near the opening of each mound. The results in Table 2.5 demonstrate that if this oscillation isn't sampled adequately, much of the upward and downward transport is missed and calculated rates of volume expulsion and subduction are underestimates.

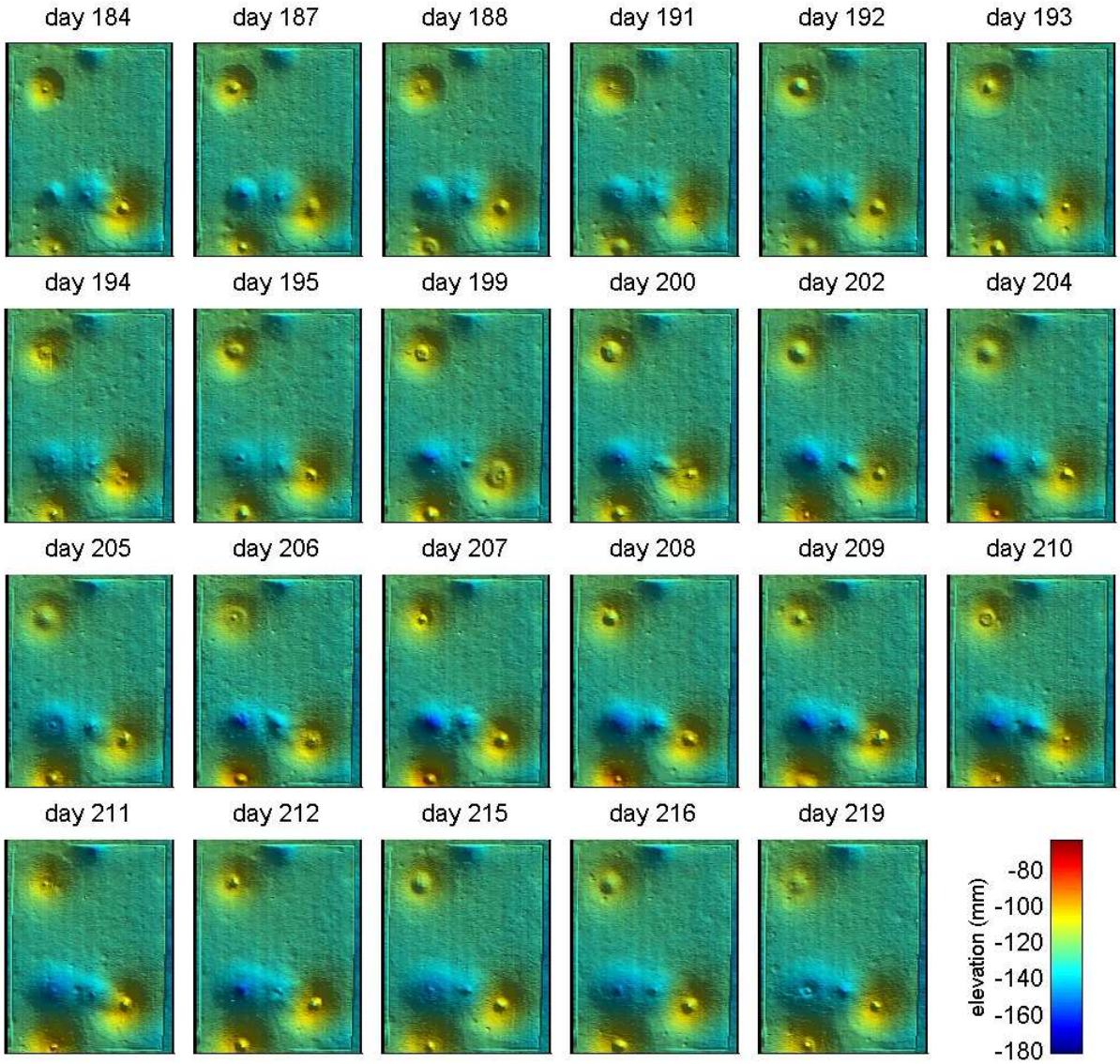

Figure 2.20 Maps of Aquarium 1 sediment surface during period of frequent scanning.

Matters are further complicated because it is likely that in the vicinity of the mound openings, the same sediment is getting shifted up and down. Some particles are oscillating rapidly between the surface and depth, while others nearby remain unmoved over the same period of time. It's clear that there is a distribution of sediment turnover rates in the sediment, and for some applications valuable information is lost if the sediment turnover is described only as an average quantity.

The nature of these experiments does not allow a good estimate of the dry mass of sediment expelled per annum, simply because volumes of sediment were measured rather than mass. As a rough guide, however, if we assume a porosity of 0.4 and a sand density of 2.65 g/cm^3, expulsion rates range from 160 to 640 g/opening/year and subduction rates range from 170 to 740 g/opening/year. The population density of *Trypaea australiensis* varies enormously. Assuming 20 burrow openings/m^2 and the

lower expulsion rate, sediment expulsion rates could be as low as 3kg/m^2/year. If there are 200 burrow openings/m^2 and the higher expulsion rate, sediment expulsion rates could be as high as 127 kg/m^2/year. Subduction rates would cover a similar range.

There are good reasons for believing that the volume rates calculated from this experiment are far lower than experienced in the field. Comparisons between field and laboratory measurements for other species of thalassinidean shrimp have revealed large differences. The following examples all used direct entrapment measurement techniques. Bird (1997) estimated sediment turnover rates for *Biffarius arenosus* in the field and found ejection rates of 4.26 g dry mass sediment/individual/day. Her earlier measurements conducted in the laboratory (using the same species) had produced a sediment turnover estimate of 0.79g dry mass/individual/day (Bird et al. (1997)). Laboratory-derived estimates for *Callianassa subterranea* are 15 kg/m^2/year (Stamhuis et al. (1997)) and 11 kg/m^2/year (Rowden et al. (1998)), yet the same methods used in the field for *Callianassa filholi* yielded a sediment turnover rate of 96 kg/m^2/year (Berkenbusch and Rowden (1999)), even though the density of *Callianassa filholi* individuals was 2.5 times lower than the density of *Callianassa subterranea* and the animals are deposit feeders of a similar size. Berkenbusch and Rowden (1999) suggested that the large difference between the two measurements reflects the fact that the *Callianassa subterranea* measurements were made in constant laboratory conditions, while the *Callianassa filholi* measurements were made *in situ* and accounted for a number of physical factors (including temperature variation, animal size and burrow position relative to the shore). Other burrowing animals in the field would encounter and damage thalassinidean burrows, so creating more burrow maintenance work for the inhabitants. Other contributing factors could be the presence of juveniles and post-larval shrimp in field studies (they were absent from the laboratory studies), and the fact that the *Callianassa filholi* measurements were made on an intertidal sandflat (the authors believe there may be a significant difference in sediment turnover rates between intertidal and subtidal populations). Berkenbusch and Rowden (1999) noted a strong seasonal variation in *Callianassa filholi* sediment turnover rates. By maintaining the laboratory at approximately 20 degrees, I removed a seasonal influence from my experiments. There has been speculation that thalassinidean sediment turnover rates are influenced by sediment nutrient content, however measurements reported by Stamhuis et al. (1997) were unable to confirm a significant effect.

2.5 *Conclusions*

The techniques employed in these experiments are more accurate than direct entrapment or mound volume estimates based on cone volume formulae. A further advantage is that the scanner detected downward as well as upward transport. Unfortunately, the animals in these experiments were restricted to laboratory aquaria which were shallower than their native sediment, and there were none of the disturbances typically experienced in the field (other burrowing macroinvertebrates, waves, tides, storms and fishing folk armed with yabby pumps). For these reasons it would be desirable to undertake a similar experiment in the field. Nevertheless, the experiments yielded useful insights into the creatures' burrowing habits, and highlighted many issues regarding turnover measurement techniques.

The experiments have demonstrated substantial downward transport of sediment, particularly once a burrow has been established. Burrow openings function as chimneys of rapid exchange between the sediment surface and depth. This mechanism is important as it would facilitate rapid transport of fresh organic matter to considerable depths in the sediment, so affecting diagenesis pathways at depth. The oscillating transport between surface and depth has not been detected by any of the conventional methods for estimating sediment transport. Further, a high sampling rate needs to be employed to detect the oscillating transport; failure to do so produces significant underestimates in the calculated expulsion and subduction rates.

These experiments have done little to constrain *Trypaea australiensis* sediment turnover estimates. Rather, they have highlighted the potential for enormous variation in estimates. Similar difficulties have been encountered in other studies. For example, Stamhuis et al. (1997) recalculated sediment turnover rates for *Callianassa subterranea* by employing additional knowledge about temperature and population density effects, and nearly trebled an earlier estimate using the same data. Work by Berkenbusch and Rowden (1999) and Rowden et al. (1998) have highlighted the sensitivity of turnover estimates to body size, temperature and overlying tidal behaviour. The most striking effect highlighted in my experiments has been the effect of downward transport and sampling frequency. I have found very little discussion on these points in the literature.

We surmise from these experiments that some sediment particles are oscillating rapidly between surface and depth, while other particles nearby are buried far more slowly, to return to the surface only after a much longer time scale. Problems in assessing the distribution of sediment turnover times and depths within the sediment

will not be resolved using any present techniques. There may be some scope for non-destructive tracer particle experiments (allowing continuous measurements rather than taking destructive cores). In particular, experiments with fluorescent particles are possible. For example, particles could be buried at depth and their arrival at the surface recorded by multiple photographs under ultra-violet radiation. Alternatively, such particles could be distributed as a layer on the surface and their subduction monitored by photographs and subsequent coring at experiment completion. Another possibility is the use of tungsten carbide labels, which can be detected under x-ray radiation.